Infrared Frequency-Modulation Probing of Cl + C_3H_4 (Allene, Propyne) Reactions: Kinetics of HCl Production from 292 to 850 K

John T. Farrell[†] **and Craig A. Taatjes***

Combustion Research Facility, Mail Stop 9055, Sandia National Laboratories, Livermore, California 94551-0969

Received: February 24, 1998; In Final Form: April 15, 1998

Absolute rate coefficients for the reactions of chlorine atoms with allene (propadiene, $H_2C{=}C{=}CH_2$) and propyne ($HC{\equiv}C{-}CH_3$) have been measured as a function of temperature (292−850 K) and pressure (4−10 Torr) with a laser photolysis/CW infrared long path absorption technique. The reactions are initiated via pulsed laser photolysis of Cl_2 and monitored through CW infrared frequency-modulation spectroscopy of the HCl product. At room temperature (292 K), the reaction of Cl with allene proceeds almost exclusively through addition, with little HCl generated through either abstraction or elimination. HCl production increases with temperature, and becomes unity at $T \geq 800$ K. Quantitative HCl yield measurements allow the contributions of addition and abstraction/elimination to the total rate to be determined. The rate coefficient for HCl production is described between 292 and 850 K by the Arrhenius expression, $k^{\text{allene}}_{\text{metathesis}}(T) = (3.7 \pm 1.7) \times 10^{-10}$ exp[−(1671 ± 286)/T] cm^3 molecule^{-1} s^{-1}, (all error bars ±2σ precision only). In contrast with the Cl + allene reaction, both addition and metathesis appear to be important channels in the reaction of Cl + propyne near room temperature. The reactions display biexponential HCl time profiles at $T \leq 400$ K, but at $T \geq 500$ K, only single-exponential evolution is observed. The HCl yield at 293 K is ≈70% and reaches unity at $T \geq 500$ K. A fit of the rate coefficient for HCl production between $400 \leq T \leq 800$ K to standard Arrhenius form gives $k^{\text{propyne}}_{\text{metathesis}}(T) = (3.7 \pm 1.0) \times 10^{-11}$ exp[−(685 ± 151)/T] cm^3 molecule^{-1} s^{-1}. The data over the whole 292−800 K temperature range exhibit curvature and are better fit by the modified Arrhenius expression (with the temperature exponent fixed at 2) $k^{\text{propyne}}_{\text{metathesis}}(T) = (1.25 \pm 0.21) \times 10^{-12}$ (T/298)^2 exp[(500 ± 93)/T] cm^3 molecule^{-1} s^{-1} (±2σ precision). Preliminary measurements are also presented for Cl + isobutene between 300 and 700 K, which were required to correct for the small butene contamination in the propyne. Measurements carried out in Ar buffer indicate that vibrationally excited HCl is formed with both allene and propyne and allow an estimate to be made for k_{VET}, the HCl(v=1) + C_3H_4 vibrational relaxation rate coefficient. In the Cl + allene reaction, approximately half ($f = 0.42 \pm 0.10$) of the HCl is formed in $v = 1$, and $k_{\text{VET}} = (2.8 \pm 0.4) \times 10^{-12}$ cm^3 molecule^{-1} s^{-1}; with propyne, the corresponding values are $f = 0.55 \pm 0.09$ and $k_{\text{VET}} = (8.6 \pm 3.6) \times 10^{-12}$ cm^3 molecule^{-1} s^{-1}. The qualitatively different dynamics for Cl + allene vs propyne can be attributed to formation of a resonantly stabilized radical with allene (chloroallyl), which greatly enhances the addition rate. Comparisons are also made with recent ab initio calculations of energies and transition states for the Cl + C_3H_4 reactions.

Introduction

The reactions of Cl atoms with small hydrocarbons play an important role in processes as diverse as the synthesis of chlorinated plastics,[1] biomass combustion,[2,3] and the incineration of CFC's, hazardous waste, and chemical weapons stockpiles.[4,5] High-quality kinetic data for these reactions, especially at elevated temperatures, are crucial for modeling these processes accurately. Although reactions of Cl with the C_{1-4} alkanes[6−12] and the simple alkenes ethylene[8,9,13−17] and propylene[18−20] have been well studied, the reactions with many other small hydrocarbons have been poorly characterized, despite their importance in the processes described above. For example, the C_3H_4 isomers allene and propyne are formed as intermediates in the combustion of saturated[21,22] and unsaturated,[23−27] hydrocarbons. In addition, propargyl radical, the resonance-stabilized product of H fission from C_3H_4, has been implicated in aromatic and soot formation during the oxidation of aliphatic hydrocarbons.[26,27] Very few data have been reported for the reactions of Cl with these species, however. Wallington et al.[28] have provided the only measurements of the rate coefficients for the reaction of Cl atoms with allene and propyne. Their experiments have shown that the Cl + C_3H_4 reactions are fast, with rate coefficients of $(4.38 \pm 0.26) \times 10^{-10}$ and $(2.68 \pm 0.16) \times 10^{-10}$ cm^3 molecule^{-1} s^{-1} for allene and propyne, respectively. The rate coefficients have been measured only at room temperature and a single pressure (760 Torr in synthetic air), and more detailed information about the reactions, such as activation energies and Arrhenius preexponential factors, has not been determined. Additionally, the earlier experiments monitored the disappearance of the hydrocarbon reactant, and consequently the relative importance of the metathesis (reaction 1) vs addition (reaction 2) channels could not be assessed.

$$\text{Cl} + \text{C}_3\text{H}_4 \xrightarrow{k_1} \text{C}_3\text{H}_3 + \text{HCl} \qquad (1)$$

$$\text{Cl} + \text{C}_3\text{H}_4\ (+\text{M}) \xrightarrow{k_2\ ([\text{M}])} \text{C}_3\text{H}_4\text{Cl}\ (+\text{M}) \qquad (2)$$

The determination of these quantities and the corresponding

[†] Sandia National Laboratories Postdoctoral Associate.
* To whom correspondence should be addressed.

S1089-5639(98)01265-1 CCC: $15.00
Published on Web 05/30/1998

greater understanding of chlorination reactions of unsaturated hydrocarbons is the motivation behind the present temperature-dependent study.

Previous studies of Cl atom reactions with unsaturated hydrocarbons have shown that the addition channel dominates near room temperature, even at modest (≈10 Torr) pressures. Both acetylene and ethylene exhibit a dramatic pressure dependence to the association rate coefficient and are in the falloff regime even at pressures of several thousand Torr.[13] The high pressure limit decreases rapidly with increasing molecular size and is below 0.25 Torr for the Cl + isoprene reaction.[29] Because the metathesis channel is endothermic for acetylene and ethylene, HCl formation is negligible at 298 K. At higher temperature, the HCl production from the Cl + ethylene reaction becomes increasingly important as stabilization of the excited adduct can no longer compete with dissociation. At $T > 500$ K and pressures of 3−10 Torr, the Cl + ethylene reaction proceeds almost exclusively through abstraction with a rate coefficient given by the Arrhenius expression $k(T) = (6.2 \pm 1.4) \times 10^{-11}\ e^{-(3400\pm450)/T}$ cm^3 molecule^{-1} s^{-1}.[17]

At temperatures of >500 K, the reaction of propylene with Cl proceeds analogously to ethylene, with HCl formation via direct abstraction the only channel observed between 3 and 10 Torr.[19] While addition becomes increasingly important at lower temperature for both ethylene and propylene, the presence of an exothermic metathesis channel with Cl + C_3H_6 leads to significant HCl production at 298 K. Time-resolved analysis of the HCl formation indicates that two primary pathways are operative at $T < 500$ K, which have been interpreted as H atom abstraction and addition−elimination. Nearly half of the HCl is produced in $v = 1$ (48 ± 6%), which suggests that direct abstraction may dominate HCl production in this reaction since HCl formation via elimination from a (partially) stabilized adduct may be expected to yield a more statistical energy distribution in the product.[30,31]

Reactions of Cl with allene and propyne could be expected to be analogous to those of ethylene and propylene based on their similar size and structure. Moreover, reactions of the two C_3H_4 isomers with Cl might be expected to proceed similarly. Identical products are obtained from the metathesis reaction of Cl with allene and propyne, i.e., HCl and propargyl. Additionally, the two isomers are nearly isoenergetic, with propyne only 1.3 kcal mol^{-1} more stable than allene. As a consequence, the metathesis reaction has comparable exothermicity ($\Delta H°_{298} = -12.84$ kcal mol^{-1} for Cl + propyne vs -14.18 kcal mol^{-1} for Cl + allene)[32,33] and would be expected to constitute a major channel for both reactants by analogy with Cl + propylene ($\Delta H°_{298} = -14.4$ kcal/mol).[32,34,35] The presence of unsaturation in both isomers suggests that Cl atom addition should compete with metathesis, at least at the lower temperature range where both ethylene and propylene exhibit facile addition.[17,19]

However, the present work shows that dramatic differences in reactivity exist between allene and propyne. The Cl + allene reactions are an order of magnitude faster than Cl + propyne at room temperature and exhibit a significantly lower HCl yield (2% vs 70%). Additionally, the addition channel constitutes an important pathway for Cl + allene up to $T \approx 800$ K, whereas with Cl + propyne it ceases to be important at $T > 400$ K for the 5−10 Torr pressures of the present experiments. The HCl temporal evolution is also different for the two isomers. Simple exponential behavior is seen in the Cl + allene reaction, indicating a single dominant channel for reaction throughout the 292−850 K range studied. In the Cl + propyne reaction, on the other hand, biexponential HCl production is seen at $T \leq$ 500 K, indicating contributions from at least two pathways to HCl formation. An Arrhenius analysis of the temperature dependence of the metathesis rate coefficients for the allene and propyne reactions gives significantly different *A* factors and activation energies and provides further evidence for different mechanistic pathways to HCl generation. The accesibility of a resonance stabilized adduct (chloroallyl) dominates the kinetics of the Cl + allene reaction and is likely the most significant cause of the reactivity differences between the two isomers.

Experimental Section

Absolute rates for the chlorine + C_3H_4 reactions are investigated using the laser photolysis/continuous wave (CW) infrared long path absorption (LP/CWIRLPA) method. A schematic diagram of the experimental setup is shown in Figure 1. The Cl atoms are generated by photolysis of Cl_2 at 355 nm (∼100 mJ/pulse) with the third harmonic output from a pulsed Nd:YAG laser. The photolysis beam traverses the long axis of a temperature-controlled slow-flow reaction cell, and the time evolution of the HCl product generated after Cl atom formation is monitored via the transient, differential attenuation of a frequency-modulated CW IR probe beam. Continuous probing allows the entire time profile to be obtained following each laser shot, and signal averaging is employed to improve signal-to-noise ratios.

The experimental apparatus incorporates features described in our previous investigations of Cl + hydrocarbon reactions,[11,17,19,36] although the present experiments use a longer reaction cell and different photolysis and IR probe lasers. The reaction cell consists of a 1.5 m long × 5 cm diameter quartz tube enclosed in a commercial ceramic-fiber heater that is capable of reaching temperatures in excess of 1200 K. Supplemental heaters are placed at each end of the cell to offset heat loss and increase the length of the cell over which the temperature profile is flat. The temperature stability in the center of the cell is ±2 K at 850 K. The high-temperature limit of 800−850 K in these experiments reflects the temperatures at which thermal degradation of the hydrocarbons/photolyte is sufficiently rapid to preclude accurate rate measurements.

A Herriott-type multipass resonator is employed to increase the optical path length and therefore the detection sensitivity. The Herriott cell uses off-axis paths in a spherical resonator, which causes the probe beam to trace out a circle of spots on each mirror while mapping out a smaller circle in the center of the cell. An attractive feature of this geometry is that it confines the pump−probe overlap region to the central region of the cell where the temperature profile is flat (see Figure 1). Consequently, the resulting signals do not include contributions from reactions initiated in cooler end regions of the cell or near the walls. The length of the overlap region is controlled by adjustment of the photolysis laser diameter, which is initially expanded via a telescope and subsequently apertured with an iris. In the present experiments, the Nd:YAG beam diameter is 25 mm, which gives an overlap region 80 cm long. The probe laser undergoes 15 traversals through the cell, leading to a total path length of 12 m. While not required for the experiments described herein, the number of passes can easily be tripled with the current experimental arrangement, leading to a concomitant 3-fold increase in optical path length.

The tunable infrared light is provided by a color-center laser which is tuned to a single HCl rovibrational transition. The relative HCl concentration is measured by the absorption on the R(6) or R(7) line of the $H^{35}Cl$ fundamental transition. In these experiments, two-tone frequency modulation[37,38] is used

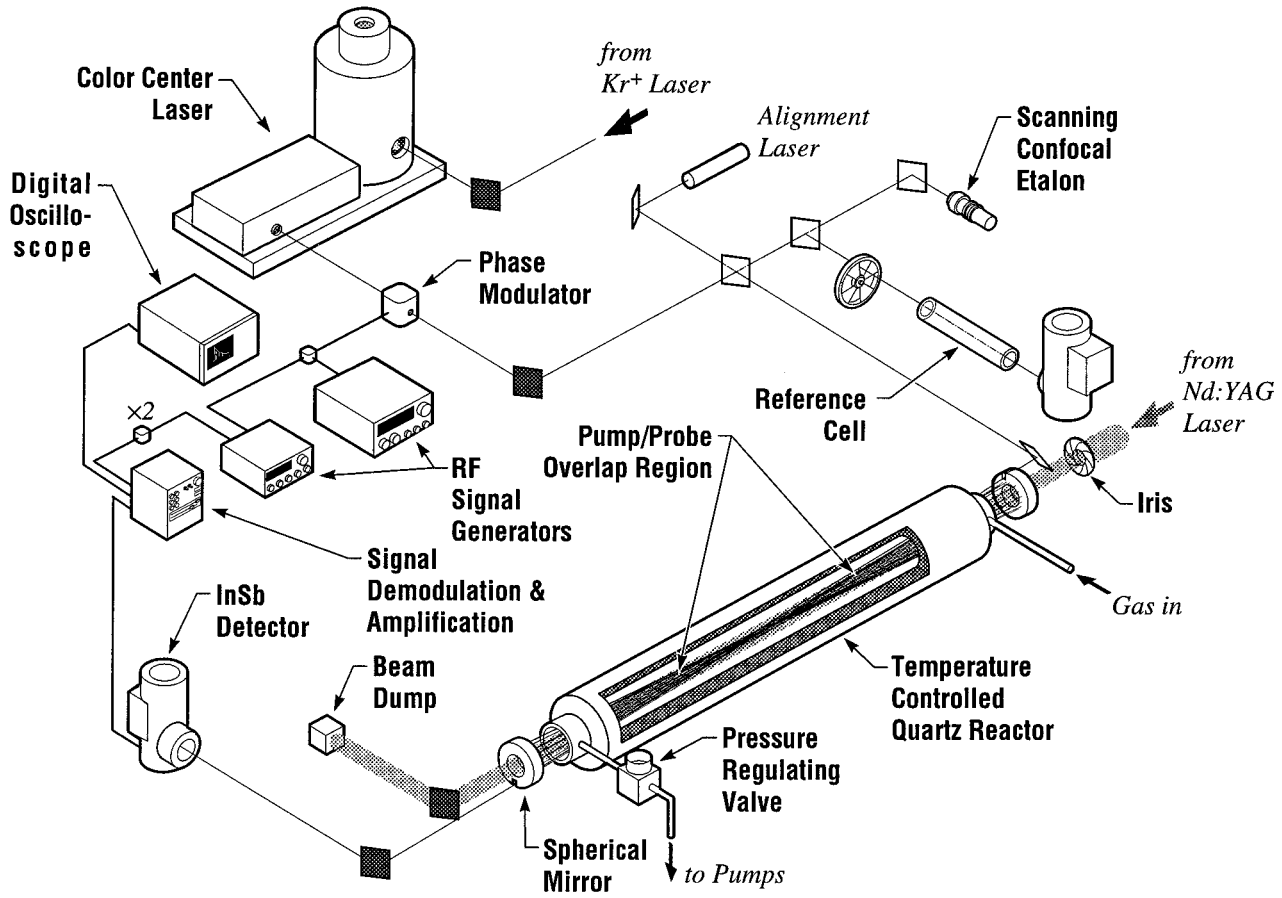

Figure 1. Schematic diagram of the laser photolysis/infrared long path absorption apparatus. The phase-modulated output of a color center laser is directed into a Herriott-type multipass cell and probes along the longitudinal axis of a temperature-controlled quartz reactor. The reflected IR beams overlap the output of a pulsed Nd:YAG laser along the central section of the cell. The transient IR absorption by the HCl product is monitored by heterodyne detection of the photocurrent from the InSb photovoltaic detector.

to improve the detection sensitivity. The infrared beam is modulated by two closely spaced radio-frequency waves (498 ± 1.1 MHz) in a $LiNbO_3$ crystal housed in an external resonant cavity. The IR beam passes through the flow cell and is monitored with an InSb photovoltaic detector. Differential attenuation of either the carrier or the sidebands unbalances the phase-modulated light and generates a beat note in the detector photocurrent whose amplitude is proportional to the absorption. The detector photocurrent is amplified and heterodyne detected at twice the intermodulation frequency (2×1.1 MHz $= 2.2$ MHz) to yield the signal. This technique has the advantage of shifting the detection frequency away from DC to a region ($\approx$ 2 MHz) where the contributions from laser amplitude and $1/f$ noise are significantly reduced. In addition, because the signal arises from a differential absorption between the carrier and sidebands, there is a significant reduction in thermal lensing noise. Thermal lensing, which is caused by the periodic probe beam steering induced by radial acoustic waves formed inside the cylindrical reaction cell following the photolysis pulse, can be a dominant noise source in pulsed photolysis experiments.

The photolyte, hydrocarbon reactant, and buffer gas flows are controlled by separate calibrated mass flow controllers. The gases enter the reactor through an inlet on the upstream end. The photolyte is 1% Cl_2 in He, and the buffer gas is either CO_2 (99.99%) or Ar (99.999%). The Cl_2 concentration is kept low enough to restrict the Cl number density to $\leq 10^{12}$ atoms/cm^3, which is 30−300-fold lower than the hydrocarbon concentration and thus facilitates operation in the pseudo-first-order limit. Allene (97%) and propyne (98.3%) were obtained commercially and used without further purification. GC/MS analysis identified propylene and propyne as the major impurities in the allene (with each present at ≈1.5%), while isobutene (2-methyl-1-propene) at 1.2% and other butenes constituted the predominant impurities in the propyne sample. Corrections to the measured rate coefficients and HCl yields due to Cl reactions with these impurities are discussed in the Results section. The flow conditions are chosen to keep the HCl absorption below 5% to maintain operation in the linear regime. The effects of secondary reactions of Cl atoms with reaction products are minimized by replenishing the reactant mixture between photolysis pulses, which constrains the photolysis laser repetition rate to 0.5−1.5 Hz for typical total flows of 1500 sccm.

One possible complication in the present study is the isomerization of allene to propyne prior to reaction with the Cl atoms. The isomerization is nearly thermoneutral, with propyne only 1.3 kcal mol^{-1} lower in energy than allene. As described above, GC/MS analysis confirmed the composition of the reagents. The isomerization rate predicted from an RRKM rate expression[39] that agrees with shock tube measurements[40] indicates that the isomerization should be insignificant even at the highest temperatures of the study ($k_{uni} \approx 10^{-3}$ s^{-1} at 850 K using $\log A = 14.03$ and $E_a = 64.311$ kcal mol^{-1} for k_∞). Even with the longest residence time used in these experiments (2 s), less than 0.2% of the allene will be lost by isomerization to propyne. The chemical integrity of the allene is supported by the very different kinetic behavior observed between Cl + allene and propyne, with the former reaction proceeding much faster than the latter and yielding a very different product distribution.

The exothermicity of the $Cl + C_3H_4 \rightarrow HCl + C_3H_3$ reactions is sufficient to populate vibrationally excited HCl. Since

absorption probes the differential population between levels, it is necessary to ensure that the absorption signals yield an accurate representation of the HCl production. The kinetic measurements are therefore carried out in CO_2 buffer gas, which is highly efficient at relaxing vibrationally excited HCl. Separate measurements are made in Ar to estimate the HCl vibrational distribution and HCl relaxation rate by C_3H_4. At room temperature, the reaction exothermicity is high enough to populate $v = 1$ of HCl (2886 cm^{-1} or 8.25 kcal mol^{-1}), but not $v = 2$ (5665 cm^{-1} or 16.2 kcal mol^{-1}). The Cl + propyne measurements in Ar are carried out at 293 K to minimize the production of HCl($v = 2$) from the high-energy tail of the Boltzmann distribution. The Cl + allene measurements required a higher temperature (600 K) where the HCl yield was sufficiently high but where production of $v = 2$ is correspondingly greater. Although direct observation of HCl $v = 2 \leftarrow 1$ transitions would provide complementary data on the HCl vibrational distribution and relaxation rate by C_3H_4, the tuning range of the color center laser does not extend to the regions where these transitions have appreciable Boltzmann populations, and access to these transitions is not feasible with the current experimental arrangement.

Measurements of the HCl yield in the Cl + C_3H_4 reactions are required to determine the abstraction rate coefficients in the presence of competing addition channels. In the present experiments, methanol ($T \leq 400$ K) or propylene ($T \geq 500$ K) is flowed alternately with the C_3H_4 through separate mass flow controllers while holding the photolysis conditions constant. The HCl yield is measured as the ratio of the transient HCl absorption signals, assuming $\phi_{HCl} = 1$ for methanol[41] and propylene[19] in the temperature ranges specified above. In the experiments conducted at $T \leq 400$ K, 50 sccm of 10% O_2 in Ar is added to the flow to suppress chain chemistry initiated by Cl + methanol reaction products.

Kinetic Analysis

The Cl + $C_3H_4 \rightarrow$ HCl + C_3H_3 reaction is exothermic for both allene ($\Delta H°_{298} = -14.2$ kcal/mol) and propyne ($\Delta H°_{298} = -12.8$ kcal/mol)[32,33] and thus may be expected to involve relatively facile metathesis. In systems such as Cl + alkanes[10−12] where HCl formation via abstraction is the only major reaction pathway, the temporal profile for HCl production is described under pseudo-first-order conditions by a single exponential, with a rise time coefficient equal to the rate for Cl atom removal, i.e.,

$$[HCl]_t = [Cl]_0(1 - e^{-k_1[alkane]t}) \quad (3)$$

In the Cl + C_3H_4 reaction, both metathesis and addition are expected to contribute to Cl atom removal, and hence the expression for temporal evolution of HCl must be modified to reflect the additional channel:

$$[HCl]_t = [Cl]_0 \frac{k_1}{k_1 + k_2}(1 - e^{-(k_1+k_2)[C_3H_4]t}) \quad (4)$$

All the temporal profiles for HCl production in the Cl + allene reaction are well described by a single exponential over the temperature range $292 \leq T \leq 850$ K. A representative HCl growth curve is shown in Figure 2. The value of ($k_1 + k_2$) is extracted as the slope from a fit of the HCl rise time vs C_3H_4 concentration as shown in Figure 3. The effective rate coefficient for the HCl producing channels, k_1, is obtained by multiplying the total rate by the measured HCl yield $\phi_{HCl} = k_1/(k_1 + k_2)$.

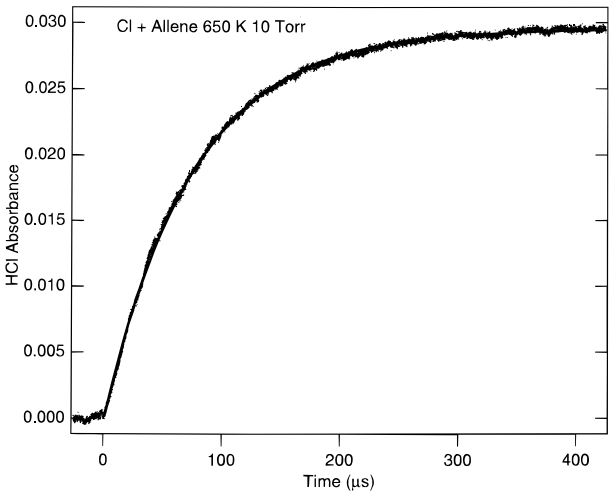

Figure 2. Representative time-resolved HCl absorption signal for the Cl + allene → HCl + propargyl reaction at 650 K and 10 Torr total pressure. The solid line is a fit to a simple exponential rise, eq 4.

In Cl atom reactions with unsaturated hydrocarbons, HCl production can also occur via an addition−elimination mechanism. The HCl temporal evolution of systems in which both abstraction and addition−elimination pathways are prominent will be biexponential if there are disparate time scales of these events.[19] Biexponential temporal behavior can also arise from a reversible addition reaction with subsequent abstraction. These two possibilities cannot be distinguished with our present experimental configuration since the resulting kinetic equations for HCl formation are the same, although simultaneous measurement of reagent depletion would differentiate between these two possibilities. Figure 4 shows a time trace for the reaction of Cl + propyne, which exhibits biexponential HCl evolution at $T \leq 400$ K. The kinetics of HCl formation due to both abstraction and addition followed by either stabilization or elimination are treated most simply by a modified Lindemann mechanism: In this mechanism, k_b is an effective rate coefficient

$$Cl + C_3H_4 \xrightarrow{k_a} HCl + C_3H_3 \quad (5)$$

$$Cl + C_3H_4 \xrightarrow{k_b} C_3H_4Cl^{\#} \begin{cases} \xrightarrow{k_E} HCl + C_3H_3 \\ \xrightarrow{k_M} C_3H_4Cl \end{cases} \quad (6)$$

for formation of an adduct that that been stabilized sufficiently that it does not dissociate back to reactants, but still has enough energy to eliminate HCl. The initial adduct formation can be rationalized as a reversible association followed by partial stabilization:

$$Cl + C_3H_4 \underset{k_{-\alpha}}{\overset{k_\alpha}{\rightleftharpoons}} C_3H_4Cl^{\#\#} \xrightarrow{k_\beta} C_3H_4Cl\# \quad (7)$$

Applying a steady-state approximation for $C_3H_4Cl^{\#\#}$ gives $k_b = k_\alpha k_\beta/(k_{-\alpha} + k_\beta)$. The kinetic equations implied by this mechanism yield a biexponential expression for the HCl concentration as a function of time:

$$HCl(t) = [Cl]_0(A - Be^{-(k_E+k_M)t} - Ce^{-(k_a+k_b)[C_3H_4]t}) \quad (8)$$

where A, B, and C are functions of the individual rate coefficients. At sufficiently long time, eq 8 reduces to HCl ($t \rightarrow \infty$) = $A[Cl]_0$, which relates A to the effective rate coefficients k_1 and k_2 by recognizing it as simply the HCl yield, i.e.,

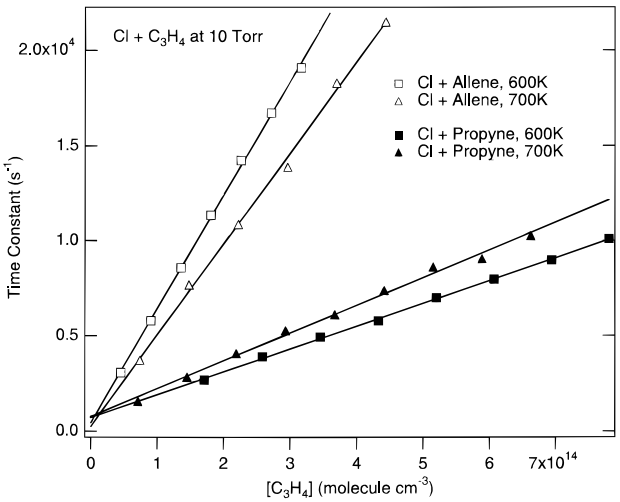

Figure 3. Measurements at 600 and 700 K of the pseudo-first-order rate coefficient, (HCl rise time)$^{-1}$ vs $[C_3H_4]$ for allene and propyne at 10 Torr. Single-exponential temporal evolution of the HCl is observed at these temperatures for both hydrocarbons. The different intercepts for the allene and propyne experiments are due to the use of different CO_2 buffer gas cylinders and reflects the contributions to the total rate from background reactions of Cl with the hydrocarbon impurities. These reactions are constant as a function of $[C_3H_4]$ and consequently do not affect the measured rates.

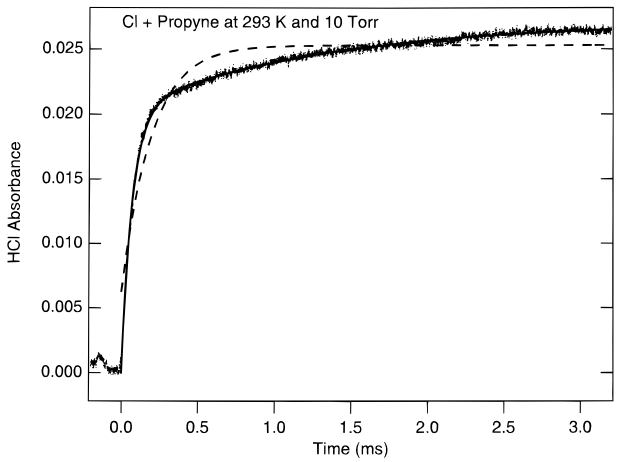

Figure 4. Representative time-resolved HCl absorption signal for the Cl + propyne → HCl + propargyl reaction at 293 K at 10 Torr total pressure. The dashed curve represents the best single-exponential fit to the data and illustrates that a simple one-step mechanism for HCl formation is not valid at this temperature. The solid curve represents a biexponential fit to the data which yields a much improved modeling of the HCl temporal evolution. The feature present at 250 μs prior to the photolysis pulse is due to electrical pickup on the detector induced by the Nd:YAG flashlamps and does not influence the data acquired after $t = 0$.

$$A \equiv \phi_{HCl} = k_1/(k_1 + k_2) \qquad (9)$$

The second term in the parentheses in eq 8 is independent of $[C_3H_4]$ and is related to the unimolecular elimination of HCl from the adduct. The final term is a function of $(k_a + k_b)$, which can be seen through inspection of eqs 1, 2 and 5, 6 to be equivalent to the total rate coefficient $(k_1 + k_2)$. The effective rate coefficients are determined by fitting a biexponential to the data and plotting the sum of the two fitted time constants vs propyne concentration. Figure 5 shows such a plot for Cl + propyne at 400 K and 10 Torr. The slope of this plot is equal to $(k_a + k_b)$, which yields k_1 when multiplied by ϕ_{HCl}, i.e., $k_1 = (k_a + k_b)\phi_{HCl}$. The figure shows that the time-resolved HCl absorption at each value of $[C_3H_4]$ is indeed composed of

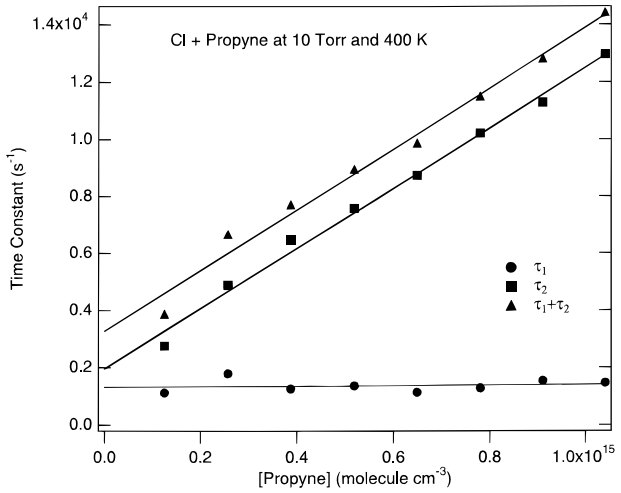

Figure 5. Rise time constants (s^{-1}) for the two biexponential time constants (● and ■) and their sum (▲) vs [propyne] at 10 Torr and 400 K. The slope of the sum yields the effective total rate coefficient while the intercept reflects excited C_3H_4Cl adduct removal and Cl loss channels such as diffusion and background reactions.

a concentration-dependent and -independent term, indicating that the steady-state assumption invoked above (eq 7) is valid for this system. Although eq 8 implies that the intercept of Figure 5 should provide an estimate of $(k_E + k_M)$, in practice the intercept also contains contributions from Cl atom removal due to diffusion and reaction with buffer gas impurities. These contributions remain constant as a function of propyne concentration, however, and thus the slope of the plot in Figure 5 provides a reliable measure of the reaction rate coefficient. Although outside the scope of this paper, a more detailed investigation of biexponential HCl production in exothermic Cl + unsaturated hydrocarbon reactions is currently underway in our laboratory. The possible role of partial adduct stabilization in an addition−elimination pathway may be amenable to study by measurement of the HCl yield and time constant for stabilization as a function of pressure and temperature.

Results

Allene. Even though hydrogen abstraction from allene by Cl is exothermic at room temperature, very little (≈2%) HCl is observed from the reaction at 292 K. The low yield makes a direct determination of the rate coefficient difficult, and consequently the rate measurements at this temperature have been carried out in the presence of methanol, which serves as the primary source of HCl. The concentration of the methanol is held constant as the allene concentration is varied, and the rate coefficient is determined as described above, with the only difference being that the intercept also includes the (zero allene) rate for Cl atom removal by methanol. At $T \geq 400$ K, the HCl yield is sufficient to permit direct rate measurements. All the temporal profiles for HCl production in the Cl + allene reaction are well described by a single exponential over the temperature range $292 \leq T \leq 850$ K. The measured rate coefficients are shown in Figure 6. Over the range 292−750 K, the total rate coefficient for Cl removal $(k_1 + k_2)$ exhibits a negative temperature dependence, which is characteristic of addition reactions. A slight pressure dependence is seen at $292 \leq T \leq 600$ K, with a larger total rate coefficient observed at 10 Torr than at 5 Torr. The faster rate at the higher pressure is accompanied by a lower HCl yield, however, and the metathesis rate coefficient given by the product of $(k_1 + k_2)\phi_{HCl}$ is constant to within experimental error. The decreasing importance of the

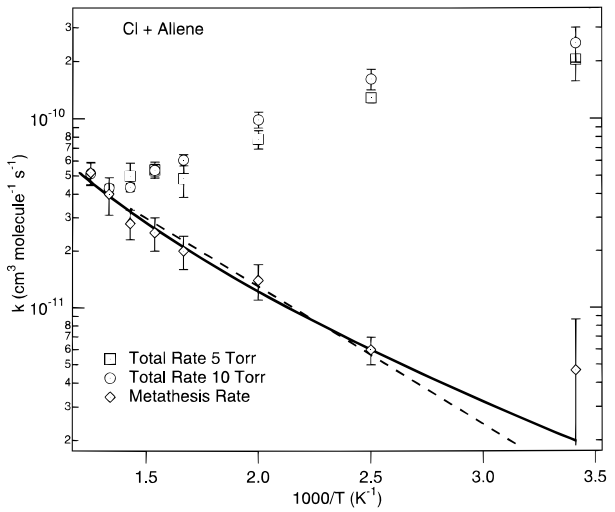

Figure 6. A semilogarithmic Arrhenius plot for the reaction Cl + allene. The squares and circles represent the total reaction rates at 5 and 10 Torr, respectively. The diamonds represent the weighted average of the HCl production rate, k_1, determined by multiplying the total rate by HCl yield. The dashed line is from a fit of k_1 using a simple Arrhenius expression, $k_{\text{metathesis}}^{\text{allene}} = (3.7 \pm 1.7) \times 10^{-10} \exp(-(1671 \pm 286)/T)$ cm^3 molecule^{-1} s^{-1}. The solid line is a fit to a modified Arrhenius expression with a temperature exponent fixed at $n = 2$, $k_{\text{metathesis}}^{\text{allene}} = (1.25 \pm 0.68) \times 10^{-11}(T/298)^2 e^{-(529\pm320)/T}$ cm^3 molecule^{-1} s^{-1}. Error bars represent $\pm 2\sigma$ precision only.

addition channel with temperature implied by the decrease in the total rate is supported by a corresponding increase in ϕ_{HCl}, from ≈0.02 at 292 K to ≈1 at $T \geq 800$ K (see Table 1).

As described in the Experimental Section, the allene used in these experiments contains propylene and propyne as contaminants, both of which will contribute to HCl production. Corrections to the measured rate coefficients and HCl yield are made at each temperature and pressure using the values for Cl + propylene[19] and Cl + propyne (this work) and the concentration of the impurities measured by GC/MS analysis. The rate corrections are all appreciably smaller than the experimental uncertainties, as are the HCl yield corrections at high temperature. At the lower temperatures investigated, the corrections are comparable to the measurement uncertainty. The uncorrected and corrected data are collected in Table 1. A weighted average of the 5 and 10 Torr data is used to calculate $k_{\text{metathesis}}^{\text{allene}} = (k_1 + k_2)\phi_{\text{HCl}}$ at each temperature; the variation with $1/T$ is shown in Figure 6. A weighted least-squares fit of the data shows that the temperature dependence of $k_{\text{metathesis}}^{\text{allene}}$ is well fit by a simple Arrhenius expression over the range $292 \leq T \leq 850$ K:

$$k_{\text{metathesis}}^{\text{allene}} = (3.7 \pm 1.7) \times 10^{-10} e^{-(1671\pm286)/T} \text{ cm}^3 \text{ molecule}^{-1} \text{ s}^{-1} \quad (10)$$

where the 2σ error limits represent the precision of the data and assume uncorrelated errors in the parameters. The metathesis rate at 292 K is the least well determined since it relies on an accurate measurement of a very small HCl yield. Nonetheless, even without including these data in the analysis, a slight curvature is evident in the Arrhenius plot. A weighted least-squares fit to a modified Arrhenius form gives

$$k_{\text{metathesis}}^{\text{allene}} = (1.25 \pm 0.68) \times 10^{-11}(T/298)^2 e^{-(529\pm320)/T} \text{ cm}^3 \text{ molecule}^{-1} \text{ s}^{-1} \quad (11)$$

The exponential dependence of (T/298) was constrained at 2.0 in the fit to reduce parameter correlation. This representation of the kinetic data leads to a 60% reduction in χ^2 compared with the standard Arrhenius model over the temperature range 400−800 K. The activation energy derived from eq 10 of 3.3 ± 0.6 kcal mol^{-1} is appreciably larger than the 0.2 ± 0.1 kcal mol^{-1} determined for the comparably exothermic Cl + propylene reaction.[19] Interestingly, the A factor extracted from the fit is approximately an order of magnitude larger than the values determined for other Cl + hydrocarbons abstraction reactions, which suggests an alternative route to HCl production in the Cl + allene reaction. These results will be discussed in more detail below.

Propyne. In contrast with allene, HCl-producing channels constitute the major pathways ($\phi_{\text{HCl}} \approx 0.7$) for the room-temperature reaction of propyne with Cl. Biexponential HCl evolution is observed at 293 K (4 and 10 Torr; see Figure 4) and 400 K (10 Torr only), which is consistent with HCl formation via both abstraction and addition−elimination pathways. At 400 K (4 Torr) and all higher temperatures investigated, only single-exponential HCl generation is observed, which implies that adduct dissociation is sufficiently fast that a steady-state approximation can be made for $C_3H_4Cl^{\#}$. The rise time constant is thus equal to the pseudo-first-order rate for Cl atom removal given in eq 3, and the rate coefficient for HCl production can be extracted directly as the product of the HCl yield and slope from a plot of the inverse of the HCl rise time vs [C_3H_4]. Table 2 shows the corrected and uncorrected data for ($k_1 + k_2$) and ϕ_{HCl}. Corrections for Cl reactions with isobutene (1.2%) have be applied using the data in Table 3. Rate measurements have not been reported for Cl + 1- and 2-butene, which constitute the remaining 0.5% impurity concentration, and consequently the necessary corrections to the rate coefficients and yields have been made using the values for Cl + isobutene. Because the Cl + butene reaction is appreciably faster than Cl + propyne (≈10× faster at 292 K, ≈4× faster at 700 K), the corrections to the rate coefficient are significant, i.e., 5−20%. The corrections to the HCl yield are ≈10% at 292 K but become negligible at $T \geq 500$ K, where the HCl yields for both propyne and isobutene are unity.

The values for ($k_1 + k_2$), ϕ_{HCl}, and by extension k_1 are qualitatively similar to those obtained for Cl + propylene.[19] The values for k_1, calculated as an average of the 4 and 10 Torr data and weighted by their individual uncertainties, are shown in Figure 7. The plot exhibits curvature and is not well-represented by a simple Arrhenius model; a weighted fit of the 400−800 K data to the standard Arrhenius form yields

$$k_{\text{metathesis}}^{\text{propyne}}(T) = (3.7 \pm 1.0) \times 10^{-11} e^{-(685\pm151)/T} \text{ cm}^3 \text{ molecule}^{-1} \text{ s}^{-1} \quad (12)$$

The preexponential factor derived from this fit is consistent with those determined for other Cl + hydrocarbon abstraction reactions, although the activation energy is somewhat larger than might be expected through comparison with the energetically similar Cl + propylene reaction,[19] for which $E_a/R \approx 90 \pm 50$. The data between 292 and 800 K are better fit with a modified Arrhenius form that takes into account the temperature dependence of the preexponential factor:

$$k_{\text{metathesis}}^{\text{propyne}}(T) = (1.25 \pm 0.21) \times 10^{-12}(T/298)^2 e^{-(500\pm93)/T} \text{ cm}^3 \text{ molecule}^{-1} \text{ s}^{-1} \quad (13)$$

The exponent of T/298 was constrained to the transition-state theory value[44] of 2.0 to reduce parameter correlation. The

TABLE 1: Rate Coefficients for the Reactions Cl + Allene → HCl + C_3H_3[e]

temp K	press. (Torr)	$k_1 + k_2$[a]	$k_1 + k_2$[a,b] (cor)	ϕ_{HCl}	ϕ_{HCl}[b] (cor)	k_1[a,c]
292						0.47 ± 0.4
	5	19.9 ± 4.7	20.4 ± 4.7			
	10	24.3 ± 5.2	24.9 ± 5.2	0.03 ± 0.02	0.02 ± 0.017	0.47 ± 0.4
400						0.6 ± 0.1[d]
	5	12.7 ± 0.8	12.9 ± 0.8	0.06 ± 0.01	0.05 ± 0.01	0.62 ± 0.14
	10	16.0 ± 2.0	16.2 ± 2.0	0.05 ± 0.01	0.04 ± 0.01	0.64 ± 0.16
500						1.4 ± 0.3[d]
	5	7.65 ± 0.87	7.80 ± 0.87	0.18 ± 0.06	0.17 ± 0.06	1.3 ± 0.5
	10	9.69 ± 0.96	9.90 ± 0.96	0.15 ± 0.05	0.14 ± 0.05	1.4 ± 0.4
600						2.0 ± 0.4[d]
	5	4.79 ± 0.99	4.85 ± 0.99	0.42 ± 0.13	0.41 ± 0.13	2.0 ± 0.5
	10	5.98 ± 0.41	6.07 ± 0.41	0.36 ± 0.15	0.35 ± 0.15	2.1 ± 0.6
650						2.5 ± 0.5[d]
	5	5.32 ± 0.54	5.39 ± 0.54	0.55 ± 0.25	0.54 ± 0.25	2.9 ± 1.4
	10	5.29 ± 0.41	5.36 ± 0.41	0.47 ± 0.10	0.46 ± 0.10	2.5 ± 0.6
700						2.8 ± 0.5[d]
	5	4.93 ± 0.86	4.99 ± 0.86	0.65 ± 0.23	0.64 ± 0.23	3.2 ± 1.3
	10	4.31 ± 0.22	4.35 ± 0.22	0.63 ± 0.14	0.62 ± 0.14	2.7 ± 0.6
750	10	4.28 ± 0.19	4.32 ± 0.19	0.93 ± 0.20	0.93 ± 0.20	4.0 ± 0.9
800	10	5.09 ± 0.71	5.15 ± 0.71	1	1	5.2 ± 0.7
850	7.5	5.41 ± 0.59	5.48 ± 0.59	1	1	5.5 ± 0.6

[a] Units of 10^{-11} cm^3 molecule^{-1} s^{-1} [b] Corrected for presence of propylene and propyne contaminants as described in the text. [c] Metathesis rate coefficient calculated as the product of ($k_1 + k_2$) and ϕ_{HCl} (corrected for impurities). [d] Weighted average of determinations at 5 and 10 Torr. [e] Stated experimental uncertainties are $\pm 2\sigma$ (precision only).

TABLE 2: Rate Coefficients for the Reactions Cl + Propyne → HCl + C_3H_3[f]

temp K	press. (Torr)	$k_1 + k_2$[a]	$k_1 + k_2$[a,b] (cor)	ϕ_{HCl}[c]	ϕ_{HCl}[b,c] (cor)	k_1[a,d]
293						7.5 ± 0.7[e]
	4.4	12.3 ± 1.3	10.6 ± 1.3	0.63 ± 0.03	0.68 ± 0.03	7.2 ± 0.9
	10	13.0 ± 1.0	10.6 ± 1.0	0.64 ± 0.06	0.74 ± 0.06	7.8 ± 1.0
400						7.0 ± 0.6[e]
	4.4	9.2 ± 0.8	7.8 ± 0.8	0.83 ± 0.13	0.86 ± 0.13	6.8 ± 0.7
	10	10.6 ± 1.0	9.3 ± 1.0	0.80 ± 0.10	0.83 ± 0.10	7.7 ± 1.3
500						9.4 ± 0.5[e]
	4.4	12.1 ± 1.3	10.9 ± 1.3	1.00 ± 0.06	1.00 ± 0.06	10.9 ± 1.3
	10	11.3 ± 0.9	10.2 ± 0.9	0.90 ± 0.04	0.89 ± 0.04	9.1 ± 0.6
600						11.9 ± 0.4[e]
	4.4	13.7 ± 1.4	12.5 ± 1.4	0.99 ± 0.05	0.99 ± 0.05	12.4 ± 1.4
	10	12.1 ± 0.4	11.0 ± 0.4	1.07 ± 0.10	1.08 ± 0.10	11.8 ± 0.4
700						14.0 ± 0.5[e]
	4.4	16.2 ± 1.0	15.1 ± 1.0			15.1 ± 1.0
	10	14.8 ± 0.6	13.6 ± 0.6			13.6 ± 0.6
800	4.4	21.3 ± 3.4	20.2 ± 3.4			20.2 ± 3.4

[a] Units of 10^{-12} cm^3 molecule^{-1} s^{-1}. [b] Corrected for presence of butene contaminants as described in the text. [c] The HCl yield is taken to be unity above 600 K. [d] Metathesis rate coefficient calculated as the product of ($k_1 + k_2$) and ϕ_{HCl} (corrected for impurities). [e] Weighted average of determinations at 4.4 and 10 Torr. [f] Stated experimental uncertainties are $\pm 2\sigma$ (precision only).

curvature evident in the data is more pronounced than with other C_3 hydrocarbons and will be discussed in more detail in the Discussion section.

Generation of Vibrationally Excited HCl. A previous study of the Cl + propylene reaction[19] found that a significant fraction of the HCl was formed vibrationally excited. Because of this, the rate measurements were carried out in CO_2 buffer to ensure rapid relaxation of the HCl vibration and hence an accurate representation of the HCl population. The kinetics of HCl production in Ar buffer, which is inefficient at relaxing HCl vibrations, must explicitly account for population of all energetically accessible vibrational levels and vibrational relaxation by the hydrocarbon reactant. Quantitative measurements of both the fraction of vibrationally excited HCl and the rate coefficient for HCl vibrational relaxation by C_3H_6 could be extracted from the data taken in Ar by constraining the rate coefficients for total HCl production to the values determined in CO_2.

Measurements of the HCl time evolution in the Cl + allene and propyne reactions also exhibit a marked difference in Ar vs CO_2 buffer. This is demonstrated explicitly for Cl + propyne in Figure 8, which shows the rise time for HCl production in Ar and CO_2 determined by probing R(6) of $v = 1 \leftarrow 0$ at 292 K. The ≈5-fold rise time reduction in Ar, which is much less efficient than CO_2 at quenching HCl vibration, indicates that a significant fraction of vibrationally excited HCl is being formed. At room temperature, the reaction exothermicities for Cl + propyne ($\Delta H°_{298} = -12.8$ kcal mol^{-1}) and allene ($\Delta H°_{298} = -14.2$ kcal mol^{-1}) are sufficiently high to populate $v = 1$ of HCl (8.25 kcal mol^{-1}), but not $v = 2$ (16.2 kcal mol^{-1}). The overall kinetics scheme is simplified by carrying out the Cl + propyne measurements in Ar at 293 K where production of HCl-($v = 2$) is energetically closed. The Cl + allene reaction, however, required measurement at a higher temperature (600 K) where the HCl yield was sufficiently high, but where production of $v = 2$ from the high-energy tail of the Boltzmann distribution is correspondingly greater; i.e., 20% of the collisions have sufficient energy at 600 K to populate $v = 2$. While the following analysis, which only accounts for HCl production in $v = 0$ and 1, provides useful insight into the mechanism for HCl formation in the Cl + C_3H_4 reactions, more reliable vibrational fractions based on measurements of transitions to

TABLE 3: Rate Coefficients for the Reactions Cl + Isobutene → HCl + C_4H_7 in CO_2 Buffer Gas[c]

temp (K)	press. (Torr)	$k_1 + k_2$[a]	ϕ_{HCl}	k_1[a]
293				3.8 ± 0.5[b]
	5	10.9 ± 1.2	0.35 ± 0.04	3.8 ± 0.6
	10	15.4 ± 1.6	0.25 ± 0.05	3.9 ± 0.9
500				7.7 ± 0.3[b]
	5	8.2 ± 0.5	1	8.2 ± 0.5
	10	7.6 ± 0.3	1	7.6 ± 0.3
700				8.3 ± 0.3[b]
	5	8.1 ± 0.6	1	8.1 ± 0.6
	10	8.4 ± 0.4	1	8.4 ± 0.4

[a] Units of 10^{-11} cm^3 molecule^{-1} s^{-1}. [b] Weighted average of determinations at 5 and 10 Torr. [c] Stated experimental uncertainties are $\pm 2\sigma$ (precision only).

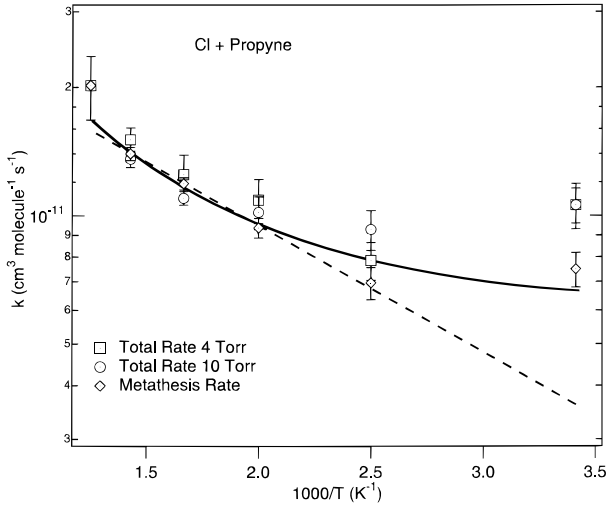

Figure 7. Arrhenius plot for k_1, the effective rate coefficient for HCl production in the Cl + propyne reaction. The squares and circles represent the total reaction rates at 4.4 and 10 Torr, respectively. The diamonds represent the weighted average of the HCl production rate, k_1, determined by multiplying the total rate by HCl yield. The values at $T \leq 500$ K are the sum of the two biexponential time constants. The dashed line is from a fit of k_1 using a simple Arrhenius expression, $k^{propyne}_{metathesis}(T) = (3.7 \pm 1.0) \times 10^{-11} \exp[-(685 \pm 151)/T]$ cm^3 molecule^{-1} s^{-1}, while the solid curve allows for a temperature-dependent preexponential factor and is given by $k^{propyne}_{metathesis}(T) = (1.25 \pm 0.21) \times 10^{-12}(T/298)^2 \exp[(500 \pm 93)/T]$ cm^3 molecule^{-1} s^{-1}. Error bars represent $\pm 2\sigma$ precision only.

all energetically accessible vibrational levels are required for a more rigorous analysis of energy partitioning in these systems.

The kinetics equations that describe the system when HCl vibrational relaxation is slow must take into account the production of HCl(v=1), and reaction 1 is therefore rewritten as

$$Cl + C_3H_4 \xrightarrow{k_1[C_3H_4]} f\,HCl(v=1) + (1-f)HCl(v=0) + C_3H_3 \quad (14)$$

where f is the fractional HCl population formed in $v = 1$. Relaxation by the Ar buffer and by the photolyte are negligible under the conditions of our experiments, and the vibrational relaxation proceeds essentially exclusively by collisions with C_3H_4.

$$HCl(v=1) \xrightarrow{k_{VET}[C_3H_4]} HCl(v=0) \quad (15)$$

In the previous study of Cl + propylene,[19] HCl formation was found to be much faster than vibrational relaxation under the conditions of the experiments, which permitted treating the initial Cl + C_3H_6 reaction as a simple step instead of the more detailed treatment outlined above. This condition also applies to the Cl + allene reaction, although it is not a valid approximation for the Cl + propyne reaction (vide infra). Analysis of the Cl + allene data in Ar buffer using the methodology outlined in ref 19 gives $f = 0.42 \pm 0.10$ and $k_{VET} = (2.8 \pm 0.4) \times 10^{-12}$ cm^3 molecule^{-1} s^{-1} at 600 K and 10 Torr. These values are quite similar to those obtained for Cl + propylene at 293 K and 10 Torr, i.e., $f = 0.48 \pm 0.06$ and $k_{VET} = (3.7 \pm 0.7) \times 10^{-12}$ cm^3 molecule^{-1} s^{-1}.

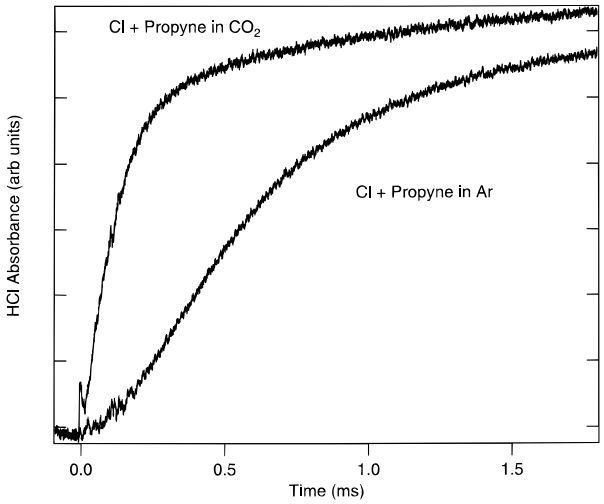

Figure 8. HCl time evolution in the reaction of Cl + propyne in Ar or CO_2 buffer at 293 K and 10 Torr total pressure. Photolyte and reactant concentrations are identical for both traces. The slower evolution in Ar is due to incomplete relaxation of the vibrationally excited HCl formed in the reaction (see text for details). The sharp feature near $t = 0$ in the CO_2 trace is due to incomplete optical filtering of the Nd:YAG photolysis pulse from the InSb detector.

For Cl + propyne, HCl formation is not sufficiently fast with respect to vibrational relaxation to employ the simplified mechanism used for Cl + allene and propylene. As evident from Figure 8, the HCl $v = 1 \leftarrow 0$ absorption profile in Ar is complicated and reflects contributions from multiple pathways. Nevertheless, analytical solutions are readily obtained to the kinetics equations described by eqs 5 and 6, which can be used to constrain the parameters in the analysis of the data taken in Ar buffer. Using these data in a fit to the kinetics equations provides $f = 0.55 \pm 0.09$ and $k_{VET} = (8.6 \pm 3.6) \times 10^{-12}$ cm^3 molecule^{-1} s^{-1} at 292 K and 10 Torr. The magnitude of f for Cl + propyne is larger than obtained with propylene or allene and reflects a higher partitioning of the reaction exothermicity as product vibrational excitation, e.g., 35 ± 10% for Cl + propyne vs 27 ± 4% (Cl + propylene) and 24 ± 8% (Cl + allene). The larger uncertainty with the C_3H_4 measurements reflects the greater uncertainty in the heat of formation of C_3H_3 (82.5 ± 3 kcal mol^{-1})[33] vs C_3H_5 (41.5 ± 0.4 kcal mol^{-1}).[34,35] While high vibrational excitation can also accompany addition−elimination, the large values of f for the reaction of Cl with allene, propylene, and propyne suggest that direct abstraction is the dominant source of HCl in the reactions of Cl with the unsaturated C_3 hydrocarbons.

Discussion

The room-temperature rate coefficient for Cl + propyne (4−10 Torr) is approximately 20-fold smaller than the value determined at 760 Torr by Wallington et al.[28] The corresponding rate decrease for Cl + allene is only a factor of 2. These

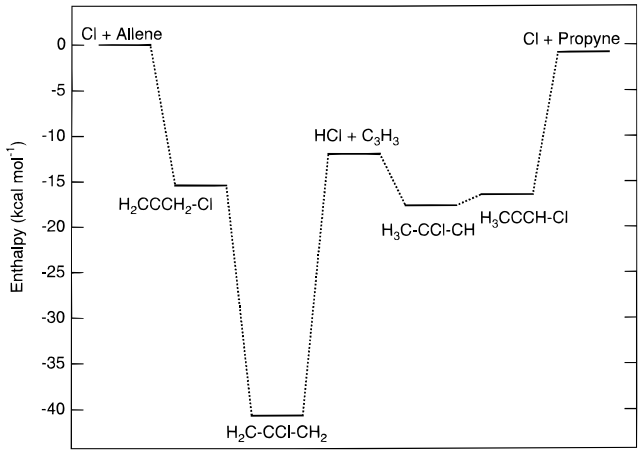

Figure 9. Calculated enthalpies for reactants, products, and adducts in the Cl + C_3H_4 → HCl + propargyl reaction from ab initio calculations.[43]

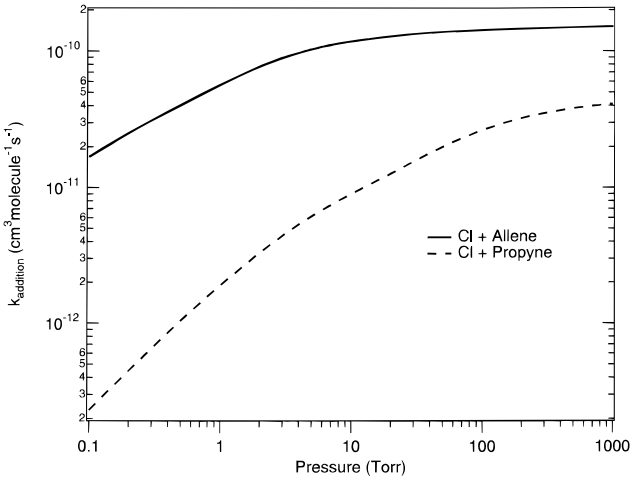

Figure 10. Calculated falloff curves for the reaction of Cl + allene and propyne at 300 K, demonstrating the more gradual decrease in association rate with allene. The differences between allene and propyne arise in part from the formation of a resonance-stabilized chloroallyl radical in the Cl + allene reaction.

values bracket the ≈ 5-fold reduction in the Cl + propylene rate over the same pressure range.[20] While a reduction in the total rate is expected at lower pressure for reactions in which addition is a dominant pathway, the 2−20-fold reduction is much smaller than observed with smaller hydrocarbons. For example, between 700 and 10 Torr the total rates at room-temperature for Cl + ethylene and acetylene differ by a factor of ≈200−300.[13] With propylene, the qualitatively different pressure behavior has been ascribed to exothermic channels corresponding to direct H atom abstraction and elimination from an incompletely stabilized adduct.[19] These channels, which are not thermodynamically accessible at room temperature for either ethylene or acetylene, dominate the reaction at low pressure and cause the rate to reach an asymptotic value. The reactions of Cl with propyne and allene have metathesis channels of comparable exothermicity to Cl + propylene, and consequently a similar limiting low-pressure rate coefficient would be expected with the C_3H_4 isomers as well.

The reduced pressure sensitivity of the total rate for reaction of Cl with the C_3 vs C_2 unsaturated hydrocarbons can also be attributed to their larger molecular size and the corresponding shift in falloff to lower pressure. The total rate for Cl + allene at 292 K shows a much smaller decrease with pressure than propylene or propyne, even though the reaction proceeds almost exclusively via addition. The differences between Cl + allene and propyne are readily understood from examination of the potential surface for the Cl + C_3H_4 reaction shown in Figure 9. The energies in this figure are based on ab initio calculations carried out at the G2 level of theory.[43] It can be seen that addition of Cl to the central carbon of allene forms the resonance-stabilized chloroallyl radical, which is predicted to lie 41 kcal mol^{-1} below the entrance channel and 29 kcal mol^{-1} below the HCl + propargyl product channel. Although our data are not sensitive to the stereoselectivity of the Cl addition, the large energy difference between addition to the central vs terminal carbon would favor addition to the former. Additionally, the relatively facile 1,2 Cl shifts and tendency of halogens to form bridged complexes with large olefins[18] suggests it is likely that Cl atoms that form incipient bonds with the terminal carbon quickly isomerize to the more stable isomer. It is thus reasonable that the formation of the highly stable chloroallyl radical accounts for the fast rate and predominance of the addition pathway even at high temperatures.

The large resonance energy available upon Cl addition to allene is not available to propyne, where addition to the terminal vs central carbon is predicted to differ by only 1.3 kcal mol^{-1}. The decreased stability of the propyne vs allene addition products evident in Figure 9 also explains the decreased importance of the addition channel. The Cl + propylene addition product, chloropropyl, is also not resonance stabilized which accounts for the similarity in the reactions of Cl with propylene and propyne.

This explanation is supported by predictions of the pressure falloff behavior for Cl + allene and propyne calculated using the simple Troe expression:[44]

$$k = \frac{k_0}{1 + k_0/k_\infty} F(k_0/k_\infty) \qquad (16)$$

Equation 16 predicts significantly different falloff behavior for Cl addition to the two C_3H_4 isomers. This is demonstrated in Figure 10, which shows falloff curves constructed using the k_0 and k_∞ values calculated according to refs 45 and 46, respectively, with the molecular and adduct properties based on ab initio calculations.[43] F_{cent} has been set to 0.5 following the observation of Kaiser and Wallington[20] of similar central broadening factors for other Cl + unsaturated hydrocarbon reactions. While the calculated high-pressure limiting rate coefficients are slightly lower than experiment (by a factor of 3−5), this simple calculation reproduces the qualitative differences between the C_3H_4 isomers, with the Cl + allene reaction displaying a more gradual falloff than Cl + propyne. The calculations predict reductions in the rate coefficient between 760 and 10 Torr by factors of 1.3 and 4.4 for Cl + allene and propyne, respectively, in modest agreement with the experimental values of 2 and 20.

Propyne. The preexponential factor for HCl-producing channels in the Cl + propyne reaction is (3.7 ± 1.0) × 10^{-11} cm^3 molecule^{-1} s^{-1}, which agrees qualitatively with the (1−2) × 10^{-11} cm^3 molecule^{-1} s^{-1} per H atom observed for other Cl + hydrocarbon metathesis reactions.[6−12] The activation energy of E_a/R = 685 ± 151 K is relatively small, yet it is significantly larger than the barriers observed for the exothermic metathesis

reactions of Cl + propylene[19] ($E_a/R = 90 \pm 50$ K) or propane,[11] where the latter rate is temperature independent between 292 and 700 K. The barrier predicted by ab initio calculations[43] is $E_a/R = 750$ K, in good agreement with the experimental value. Comparison of the propane, propylene, and propyne data suggests that increasing the hybridization of the carbon adjacent to the methyl group correlates with a slight increase in abstraction barrier. It is interesting to note that the barrier for the comparably exothermic Cl + CH_3CN reaction ($\Delta H°_{298} = -12.3$ kcal mol^{-1})[32] is larger still, i.e., 4.3 kcal mol^{-1}.[47]

A simple Arrhenius analysis of the HCl-producing channels in the Cl + propyne reaction (Figure 7) exhibits discernible curvature in the preexponential factor between 292 and 800 K. This is in contrast with the Cl + propylene[19] and propane[11] reactions, where no curvature was observed. The rate increase at higher temperature cannot be explained in the present experiment by reactions initiated by thermal decomposition of the photolyte, since the resulting (constant) HCl distribution would not depend on propyne concentration and thus would not be evident in the plots of inverse rise time vs hydrocarbon concentration. Contributions due to products of secondary radical−radical recombination also appear unlikely, since reactions of Cl with either the cyclic or linear C_6H_6 isomers would have to be orders of magnitude faster than the already rapid reaction with propyne in order to contribute. Reactions due to buffer gas contaminants would only be reflected in the intercept of the inverse rise time vs concentration plots, since they would not vary with the concentration of the primary reactant. It is also impossible that an increase at higher temperature is due to Cl reactions with the butene contaminants in the propyne; such reactions would have to have a very steep temperature dependence and unrealistic rate coefficients $\approx 1 \times 10^{-9}$ cm^3 molecule^{-1} s^{-1} at $T \approx 800$ K to account for the observed curvature. The rate coefficients for the reaction of Cl with isobutene (the major contaminant in propyne) are reported here and exhibit no such unusual behavior.

Deviation from simple Arrhenius behavior has been observed in systems that exhibit state specific rate constants.[42,48] Because the spin−orbit splitting between the $^2P_{3/2}$ ground state (Cl) and $^2P_{1/2}$ excited state (Cl*) of chlorine is 882 cm^{-1}, a significant thermal population of the excited state will exist at the higher temperatures of this study. An accelerated rate for Cl* vs Cl with hydrocarbons has been hypothesized in the Cl + methane reaction,[7] and was considered as a source of curvature in the Arrhenius plot for Cl + ethane.[11] In the latter case, however, the preexponential factor for the Cl* reaction required to reproduce the high-temperature curvature was 3−4 times larger than a normal gas-kinetic collision rate and thus was deemed unlikely to be responsible. A similar analysis for Cl + propyne, using the data between 400 and 600 K to establish the baseline rate expression for reaction with the $^2P_{3/2}$ ground state ($k = 3.0 \times 10^{-11} \exp(-537/T)$ cm^3 molecule^{-1} s^{-1}), gives a preexponential factor and E_a/R for Cl* + propyne of $\approx 1 \times 10^{-9}$ cm^3 molecule^{-1} s^{-1} and ≈3840 K. The preexponential factor in this instance is also unrealistically large and suggests that reactions of spin−orbit excited Cl atoms are not responsible for the observed curvature in the Cl + propyne Arrhenius plot.

The differences in the temperature dependence of the heat capacities of the reactants and the transition state provide a thermodynamic rationalization of non-Arrhenius behavior.[42,49] The temperature dependence of the preexponential factor can be treated very conveniently via the transition-state theory expression for the rate coefficient[42]

$$k(T) = \frac{k_B T}{h}\left(\frac{Q^\dagger}{Q_A Q_B}\right) e^{-E_0/k_B T} \qquad (17)$$

where $Q^\dagger$, Q_A, and Q_B are the partition functions for the transition state, Cl, and C_3H_4, respectively. The reactant and transition-state partition functions can be calculated over the temperature range 300−800 K using vibrational frequencies and rotational constants from ab initio calculations.[43] An Arrhenius plot of the corresponding rate coefficient calculated using eq 17 shows curvature for Cl + propyne. A fit of the predicted rate coefficient to the expression $k = A(T/298)^n \exp(-E/kT)$ gives $n = 2.9$, in good qualitative agreement with experiment. It may be useful to extend the ab initio and transition-state calculations to Cl + propylene and propane, to see whether the corresponding lack of curvature is recovered by the calculations. In addition, a more rigorous theoretical study of the potential surface for this reaction would help to shed light on the nature of the temperature dependence of the rate coefficient.

Allene. The temperature dependence of the metathesis rate coefficient in the Cl + allene reaction is moderately well fit by a simple Arrhenius form of $k = (3.7 \pm 1.7) \times 10^{-10} \exp(-1671 \pm 286)$. The most notable deviation from linearity in the plot is the rate for HCl formation at 292 K, which due to the very low HCl yield has a higher overall uncertainty. The error estimates given reflect only the precision of the determinations of the metathesis rate coefficient. Especially at very low ϕ_{HCl}, small systematic errors in the yield determination arising from, for example, background HCl production from impurities in the buffer or other trace contaminants can significantly affect the measured rate coefficient. Between 400 and 800 K, the Arrhenius plot for HCl production exhibits slight upward curvature. The rate coefficients calculated for Cl + allene using eq 17 using ab initio frequencies and rotational constants predict a $(T/298)^{2.4}$ dependence between 300 and 800 K. While the magnitude of n and the reduced curvature with respect to Cl + propyne is also in good agreement with experiment, more detailed calculations are needed to definitively attribute the curvature to the temperature dependence of the partition function ratio. The activation energy of 3.3 ± 0.6 kcal mol^{-1} obtained from a weighted fit of the data to a simple Arrhenius form is qualitatively reproduced by ab initio calculations, which predict a 2.5 kcal mol^{-1} barrier.[43] The magnitude of the barrier is significantly larger than observed for the exothermic reactions of Cl + propane, propylene, or propyne. As discussed for propyne, however, the barriers are likely sensitive to the hybridization of the nearby carbon atoms, and the unique hybridization of allene could give rise to a characteristically higher abstraction barrier. It is interesting to note that formation of the planar propargyl radical requires rotation of the orbital containing the unpaired electron by 90° in order to achieve resonance. Evidence from studies of free radical addition to allene corroborates the intuition that formation of the resonance stabilized allylic radical requires a similar rotation.[50] One posited effect of this required rehybridization is a smaller influence of the resonance energy on the energetics of the transition state than if no such geometric constraint existed. Experimental characterization of other radicals with allene would offer interesting supporting evidence of the magnitude of these effects.

The decrease in total rate with temperature observed with Cl + allene is consistent with a reaction dominated by addition. Similarly, the relatively small barrier for HCl production and large fraction of vibrationally excited HCl produced are also consistent with a direct abstraction mechanism. The preexpo-

nential factor of $(3.7 \pm 1.7) \times 10^{-10}$ cm^3 molecule^{-1} s^{-1} is an order of magnitude larger than the values typically observed for Cl + hydrocarbon abstraction reactions, however, and is instead consistent with a capture-limited reaction. Attributing the observed preexponential factor to an abstraction process would require an abnormally loose abstraction transition state, while ab initio calculations show comparable C−H−Cl bond lengths for the Cl + allene and propyne abstraction transition states.[43]

Another possible explanation that is consistent with the large *A* factor is that an addition−elimination mechanism dominates the metathesis over the entire temperature region. Because of the competition between stabilization and elimination, an effective activation energy could exist for the HCl production. It is interesting to note that the fraction of vibrationally excited HCl produced in the Cl + allene reaction (42 ± 10%) is smaller than for propylene and propyne, and was measured at higher temperature (600 K) where contributions from $v = 2$ may be greater. Thus, the relatively high degree of HCl vibrational excitation may not be inconsistent with addition−elimination mechanism if the potential surface efficiently couples vibrational energy into the HCl at the transition state. Measurement at higher pressures might help to characterize better the mechanism for HCl production in the Cl + allene reaction, and modifications to the experimental apparatus are currently underway to facilitate such measurements.

Conclusions

Absolute rate coefficients have been measured for the reactions of chlorine atoms with allene and propyne between 292 and 850 K and 4−10 Torr. The reaction of Cl with allene is dominated at low temperature by addition, driven by formation of the resonance-stabilized chloroallyl radical. Formation of HCl, which accounts for only ≈2% of the reactivity at 292 K, increases in importance with temperature and is the dominant pathway at temperatures of >800 K. Although the data for allene are consistent with HCl formation via abstraction, the preexponential factor extracted from an Arrhenius plot is an order of magnitude larger than observed with other exothermic Cl + hydrocarbons metathesis reactions, which suggests that addition−elimination may be the dominant mechanism for HCl production. With Cl + propyne, biexponential HCl temporal evolution is observed at $292 \leq T \leq 400$ K, which is consistent with production via both abstraction and addition−elimination pathways. At $T \geq 500$ K, the unity HCl yield and single-exponential HCl time evolution indicate that abstraction constitutes the major reactive pathway. An Arrhenius plot of the rate for HCl production exhibits curvature and a barrier (1.4 ± 0.3 kcal mol^{-1}) slightly larger than for Cl reactions with propylene and propane. Approximately half the HCl generated from reaction of Cl with allene and propyne is produced in $v_{HCl} = 1$, implicating the role of direct abstraction as the pathway for HCl formation.

Acknowledgment. The authors thank Leonard Jusinski for his expert technical assistance. This work is supported by the Division of Chemical Sciences, the Office of Basic Energy Sciences, the U.S. Department of Energy.

References and Notes

(1) Tirtowidjojo, M. M.; Colegrove, B. T.; Durant, J. L. *Ind. Eng. Chem. Res.* **1995**, *34*, 4202.

(2) Crutzen, P. J.; Heidt, L. E.; Krasnec, J. P.; Pollock, W. H.; Seiler, W. *Nature* **1979**, *282*, 253.

(3) Obernberger, I.; Biedermann, F.; Widmann, R.; Riedl, R. *Biomass Bioenergy* **1997**, *12*, 211.

(4) Tsang, W. *Combust. Sci. Technol.* **1990**, *74*, 99.

(5) Frenklach, M. *Combust. Sci. Technol.* **1990**, *74*, 283.

(6) Zahniser, M. S.; Berquist, B. M.; Kaufman, F. *Int. J. Chem. Kinet.* **1978**, *10*, 15.

(7) Ravishankara, A. R.; Wine, P. H. *J. Chem. Phys.* **1980**, *72*, 25.

(8) Dobis, O.; Benson, S. W. *J. Am. Chem. Soc.* **1990**, *112*, 1023.

(9) Dobis, O.; Benson, S. W. *J. Am. Chem. Soc.* **1991**, *113*, 6377.

(10) Beichert, P.; Wingen, L.; Lee, J.; Vogt, R.; Ezell, M. J.; Ragains, M.; Neavyn, R.; Finlayson-Pitts, B. J. *J. Phys. Chem.* **1995**, *99*, 13156.

(11) Pilgrim, J. S.; McIlroy, A.; Taatjes, C. A. *J. Phys. Chem. A* **1997**, *101*, 1873.

(12) Tyndall, G. S.; Orlando, J. J.; Wallington, T. J.; Dill, M.; Kaiser, E. W. *Int. J. Chem. Kinet.* **1997**, *29*, 43.

(13) Wallington, T. J.; Andino, J. M.; Lorkovic, I. M.; Kaiser, E. W.; Marston, G. *J. Phys. Chem.* **1990**, *94*, 3644.

(14) Parmar, S. S.; Benson, S. W. *J. Phys. Chem.* **1988**, *92*, 2652.

(15) Lee, F. S. C.; Rowland, F. S. *J. Phys. Chem.* **1977**, *81*, 1235.

(16) Kaiser, E. W.; Wallington, T. J. *J. Phys. Chem.* **1996**, *100*, 4111.

(17) Pilgrim, J. S.; Taatjes, C. A. *J. Phys. Chem. A.* **1997**, *101*, 4172, 8741.

(18) Lee, F. S. C.; Rowland, F. S. *J. Phys. Chem.* **1977**, *81*, 1222.

(19) Pilgrim, J. S.; Taatjes, C. A. *J. Phys. Chem.* **1997**, *101*, 5776.

(20) Kaiser, E. W.; Wallington, T. J. *J. Phys. Chem.* **1996**, *100*, 9788.

(21) McEnally, C. S.; Pfefferle, L. D. *Combust. Sci. Technol.* **1996**, *116*, 183.

(22) Dagaut, P.; Cathonnet, M.; Boettner, J. C. *Int. J. Chem. Kinet.* **1992**, *24*, 813.

(23) Homann, K. H.; Schweinfurth, H. *Ber. Bunsen-Ges. Phys. Chem.* **1981**, *85*, 569.

(24) Thomas, S. D.; Bhargava, A.; Westmoreland, P. R.; Lindstedt, R. P.; Skevis, G. *Bull. Soc. Chim. Belg.* **1996**, *105*, 501.

(25) Bittner, J. D.; Howard, J. B. *18th Symp.* (*Int.*) *Combust.* **1981**, 1105.

(26) Miller, J. A.; Melius, C. F. *Combust. Flame* **1992**, *91*, 21.

(27) Frenklach, M.; Taki, S.; Durgaprasad, M. B.; Matula, R. A. *Combust. Flame* **1983**, *54*, 81.

(28) Wallington, T. J.; Skewes, L. M.; Siegl, W. O. J. *Photochem. Photobiol. A: Chem.* **1988**, *45*, 167.

(29) Bedjanian, Y.; Laverdet, G.; Le Bras, G. *J. Phys. Chem. A* **1998**, *102*, 953.

(30) Arunan, E.; Wategaonkar, S. J.; Setser, D. W. *J. Phys. Chem.* **1991**, *95*, 1539.

(31) Arunan, E.; Rengarajan, R.; Setser, D. W. *Can J. Chem.* **1994**, *72*, 568.

(32) Pedley, J. B.; Naylor, R. D.; Kirby, S. P. *Thermochemical Data of Organic Compounds*, 2nd ed.; Chapman and Hall: London, 1986.

(33) Robinson, M. S.; Polak, M. L.; Bierbaum, V. M.; DePuy, C. H.; Lineberger, W. C. *J. Am. Chem. Soc.* **1995**, *117*, 6766.

(34) Wenthold, P. G.; Polak, M. L.; Lineberger, W. C. *J. Phys. Chem.* **1996**, *100*, 6920.

(35) Ellison, G. B.; Davico, G. E.; Bierbaum, V. M.; DePuy, C. H. *Int. J. Mass Spectrom. Ion Processes* **1996**, *156*, 109.

(36) Pilgrim, J. S.; Jennings, R. T.; Taatjes, C. A. *Rev. Sci. Instrum.* **1997**, *68*, 1875.

(37) Avetisov, V. G.; Kauranen, P. *Appl. Opt.* **1996**, *35*, 4705.

(38) Cooper, D. E.; Warren, R. E. *J. Opt. Soc. Am. B* **1987**, *4*, 470.

(39) Kiefer, J. H.; Kumaran, S. S.; Mudipalli, P. S. *Chem. Phys. Lett.* **1994**, 224, 51.

(40) Hidaka, Y.; Chimori, T.; Suga, M. *Chem. Phys. Lett.* **1985**, *119*, 435.

(41) Dobe, S.; Otting, M.; Temps, F.; Wagner, H. Gg.; Ziemer, H. *Ber. Bunsen-Ges. Phys. Chem.* **1993**, *97*, 877.

(42) Fontijn, A.; Zellner, R. In *Reactions of Small Transient Species*; Fontijn, A., Clyne, M. A. A., Eds.; Academic Press: New York, 1983.

(43) Farrell, J. T.; Durant, J. L., manuscript in preparation.

(44) Gilbert, R. G.; Luther, K.; Troe, J. *Ber. Bunsen-Ges. Phys. Chem.* **1983**, *87*, 169.

(45) Quack, M.; Troe, J. *Ber. Bunsen-Ges. Phys. Chem.* **1977**, *81*, 329.

(46) Troe, J. *J. Chem. Phys.* **1977**, *66*, 4758.

(47) Tyndall, G. S.; Orlando, J. J.; Wallington, T. J.; Sehested, J.; Nielsen, O. J. *J. Phys. Chem.* **1996**, *100*, 660.

(48) Zellner, R.; Steinert, W. *Chem. Phys. Lett.* **1981**, *81*, 568.

(49) Zellner, R. In *Combustion Chemistry*; Gardiner, W. C., Ed.; Springer-Verlag: Berlin, 1984.

(50) Byrd, L. R.; Caserio, M. J. *J. Org. Chem.* **1972**, *24*, 3881.